Journal of Photochemistry and Photobiology A: Chemistry 135 (2000) 235–240

Journal of Photochemistry and Photobiology A:Chemistry

www.elsevier.nl/locate/jphotochem

Photosensitization of nanocrystalline TiO_2 electrodes by squarylium cyanine incorporated with a ruthenium bipyridyl complex

Dongshe Zhang [a], Weibo Wang [a], Yao Liu [a], Xurui Xiao [a,*], Wei Zhao [b], Baowen Zhang [b], Yi Cao [b]

[a] *Center for Molecular Sciences, Institute of Chemistry, The Chinese Academy of Sciences, Beijing, 100080, China*
[b] *Institute of Photographic Chemistry, The Chinese Academy of Sciences, Beijing 100101, China*

Received 17 January 2000; received in revised form 7 April 2000; accepted 18 April 2000

Abstract

Photosensitization of nanocrystalline TiO_2 electrodes by adsorbing squarylium cyanine (SQ) and a mixture of squarylium cyanine and ruthenium bipyridyl complex ($RuL_2(NCS)_2$) has been investigated. Photocurrent generation from the monomers and H-type aggregates of squarylium cyanine were observed in the action spectra of squarylium cyanine sensitized electrodes. Adsorption of mixtures of squarylium cyanine and ruthenium bipyridyl complex on nanocrystalline TiO_2 electrodes was studied by absorption and infrared spectra. An association effect of photosensitization was observed in mixtures with molar proportions ($SQ:RuL_2(NCS)_2$) of 1:20, 1:50 and 1:100 mol/mol, resulting in the increase of the photoelectric response. Electron transfer mechanism was suggested in terms of quenching the fluorescence of squarylium cyanine by the presence of ruthenium bipyridyl complex and TiO_2 colloids. © 2000 Elsevier Science S.A. All rights reserved.

Keywords: Photosensitization; Squarylium cyanine; Ruthenium bipyridyl complex; Nanocrystalline TiO_2 electrodes; Photoelectric response

1. Introduction

Photosensitization of semiconductor electrodes has been studied extensively in the photoelectrochemical energy conversion. A number of organic dyes have been used as photosensitizers which harvest the light energy and transfer electrons from their excited states to the conduction band of semiconductor resulting in generating photocurrents [1–3]. The light harvesting efficiencies of photosensitizers and the interfacial electron transfer processes are of importance in determining the photosensitization efficiencies. Recently, considerable interest was generated in the study of photosensitization of nanostructured semiconductor electrodes [4–6]. In this system, very high photosensitization efficiencies were obtained by covering the large surface of nanostructured semiconductors with a monolayer of the dye. Studies of dye photosensitization of nanostructured semiconductor systems have led to the development of a new class of organic-semiconductor composite photoelectric materials for the light energy conversion applications.

Squarylium cyanine dyes have been widely used as organic photoconductors in imaging and xerography technologies [7–9]. It can also act as the efficient photosensitizers due to the possession of strong and intense absorption band in the visible and near-infrared region [10,11]. In this work, a new squarylium cyanine compound for adsorbing onto the nanocrystalline TiO_2 electrodes was synthesized. Photosensitization of nanocrystalline TiO_2 electrodes by this squarylium cyanine compound and its associated effects with ruthenium bipyridyl complex were studied.

2. Experimental details

2.1. Synthesis of organic dyes

2,3,3-Trimethyl indolenine was obtained by a one-step Fischer indole synthesis [12,13], including reaction of phenylhydrazine with methyl isopropyl ketone which led to in situ formation of phenylhydrazone under acidic conditions. By heating 2,3,3-trimethyl indolenine with propane sultone, N-R-2,3,3-trimethyl indolenine quaternary salts ($R{=}(CH_2)_3SO_3^-$) was produced. Squaric acid was prepared from hexachlorobutadiene and morpholine using methods available in the literature [14] via the one-pot method in a three-step reaction of substitution, cyclization (intramolecular ‘2+2’ addition) and hydrolysis. Squarylium cyanine compound (SQ, shown in Scheme 1) was synthesized by condensation of N-R-2,3,3-trimethyl indolenine quaternary

---

* Corresponding author. Tel.: +86-10-64888162; fax: +86-10-64879375.
E-mail address: g211@ipc.ac.cn (X. Xiao)

PII: S1010-6030(00)00291-4

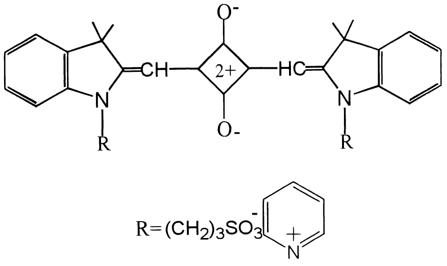

Scheme 1.

salts ($R=(CH_2)_3SO_3^-$) with squaric acid on azeotropic removal of the water of reaction in butanol/toluene mixture solvents using pyridine as the catalyst [15]. All the target products were characterized by UV, IR, MS and ^1H NMR spectroscopies.

cis-Ru[4,4′-(LL)]$_2$(NCS)$_2$(L=2,2′-bipyridyl-4,4′dicarboxylate) was synthesized using a previously described procedure [16].

2.2. Preparation of nanocrystalline TiO_2 electrodes

Colloidal TiO_2 suspension was prepared firstly by hydrolysis of titanium isopropoxide (Aldrich, 97%) in pH=1 aqueous solution under vigorous stirring in 80°C for 8 h, then autoclaved at 230°C for 12 h and evaporated in a rotary evaporator to obtain 12 wt.% colloidal TiO_2 suspension solution. After ultrasonic dispersion with the addition of carbowax (M-20,000), nanocrystalline TiO_2 electrodes were formed by spreading the colloidal TiO_2 suspension on the SnO_2 conducting glass (fluorine-doped, 30 Ω/□) and then sintered to 450°C in air for 30 min. TiO_2 crystalline grains in anatase interconnected to construct a three-dimensional network structural nanocrystalline nanoporous electrodes having a mean size of 12 nm. Electrode thickness was ~8 μm determined by Tencor α-step profilometer

2.3. Adsorption of nanocrystalline TiO_2 electrodes with organic dyes

For the adsorption of dyes, an ethanol solution containing 5×10^{-4} M SQ or mixtures of SQ and $RuL_2(NCS)_2$ in different molar proportions were prepared. Freshly prepared nanocrystalline TiO_2 electrodes, while still warm (~80°C), were dipped into the dye ethanol solution and then stored in this solution overnight. The TiO_2 electrodes became dark red. Excess dye was removed by subsequent rinsing with ethanol. The dye adsorbed nanocrystalline TiO_2 electrodes were stored in a desiccator before measurements.

2.4. Spectral measurements

Absorption spectra were recorded by using a Lambda Bio 20 spectrophotometer, the spectral resolution being 1 nm^{-1}. Infrared spectra experiments were performed on an FTIR spectrometer (FTS-165). FTIR spectra of dye molecules adsorbed on TiO_2 electrodes were measured by using KBr pellets in transmission mode with spectral resolution of 2 cm^{-1}. Fluorescence spectra were obtained on a Hitachi F-4500 fluorescence spectrophotometer equipped with Xenon lamp, the spectral resolution being 0.2 nm. All measurements were performed at room temperature.

2.5. Photoelectrochemical measurements

Photoelectrochemical measurements were carried out in a thin layer cell assembled by placing dye-sensitized nanocrystalline TiO_2 electrodes as working electrode on the top of the platinized SnO_2 conducting glass counter electrode and soaked in a thin layer of electrolyte of 0.5 M KI, 0.05 M I_2 and the mixture of ethylene and propylene carbonate (Volume ratio: 8:2).

A 250-W halogen lamp was used as the light source, (infrared) radiation was moved by 10-cm 0.01 M $CuSO_4$ solution filter. The incident light intensity was 60 mW/cm^2. A 450-W xenon lamp served as a light source for measuring photocurrent action spectra. A monochromator (WRG-1) was used to generate monochromatic light. Open circuit photovoltages and short-circuit photocurrents were recorded with a 179 digital multimeter.

3. Results and discussion

3.1. Absorption characteristic and photoelectric response of SQ sensitized nanocrystalline TiO_2 electrodes

Squarylium cyanine with substituent $(CH_2)_3SO_3^-Py^+$ shown in Scheme 1 was designed and synthesized for sensitizing nanocrystalline TiO_2 electrodes. Photosensitization was performed by building up electric coupling under the interaction of an adsorption group ($(CH_2)_3SO_3^-Py^+$) with nanocrystalline TiO_2 electrodes surface.

Fig. 1 shows the absorption spectra of SQ in ethanol solution. The major absorption bands with maximums at 636-nm wavelength, corresponding to the absorption of monomers [17], are observed. Absorption spectra of SQ on nanocrystalline TiO_2 electrodes at different adsorption times are illustrated in Fig. 2. Two absorption bands were formed at maximums of 646 and 603 nm after adsorption time of 15 min. Both absorption bands increased with extending the adsorption times and the absorption maximums did not shift appreciably during the adsorption times of 480 min. The absorption bands at 646 nm are the result of the monomeric absorption which are shifted toward the red compared with the monomeric absorption bands at the absorption spectra in ethanol solution. The absorption bands of 603 nm probably can be attributed to the formation of H-type aggregates which have energy levels higher than the monomer excited states causing a blue shift in the

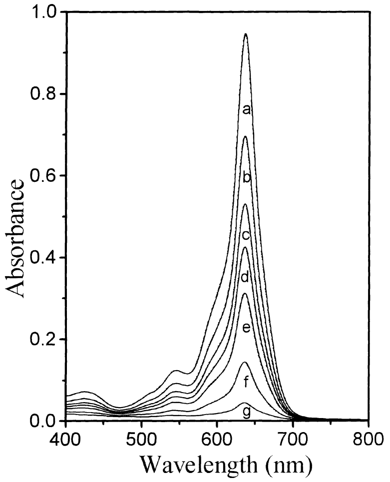

Fig. 1. Absorption spectra of SQ in ethanol solution with different concentrations: (a) 18.80; (b) 10.50; (c) 8.00; (d) 5.50; (e) 3.83; (f) 1.33; and (g) 0.50×10^{-6} M.

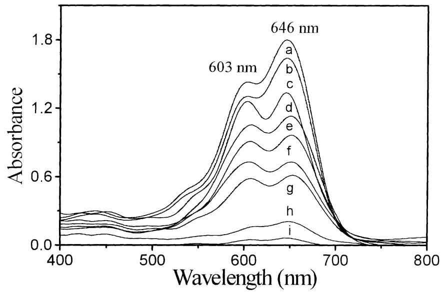

Fig. 2. Absorption spectra of SQ adsorbed on nanocrystalline TiO_2 electrodes at different adsorption times: (a) 480; (b) 240; (c) 120; (d) 60; (e) 45; (f) 30; (g) 15; (h) 5; and (i) 1 min. $C_{SQ}=0.5\times10^{-3}$ M.

absorption bands [18]. This result indicates that the adsorbed SQ molecules underwent aggregation to form H-type aggregates on the TiO_2 electrode. The formation of J-type aggregates which display a red shift in the absorption band is not observed in this spectra.

Fig. 3 shows the photocurrent action spectrum of SQ sensitized nonacrystalline TiO_2 electrodes. The absorption spectrum of SQ on TiO_2 electrode is also presented for comparison. As seen from this figure, the incident photon to current efficiency (IPCE) in the action spectrum coincides with the absorption spectrum of SQ on TiO_2 electrodes indicating that SQ is responsible for the photocurrent generation. Two photocurrent peaks observed in the action spectrum are the result of spectral sensitization of the nanocrystalline TiO_2 electrodes by the monomers and H-type aggregates of SQ. From Fig. 3, it is demonstrated that H-type aggregates of SQ can also transfer electrons to the conduction band of TiO_2 and produce the photocurrents during the photosensitization processes.

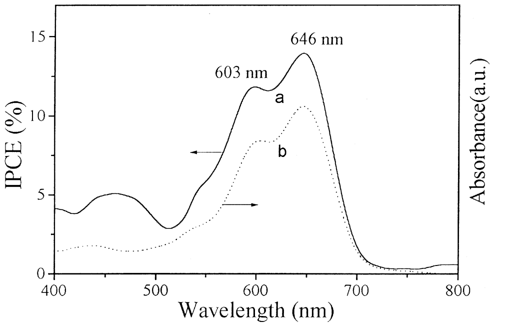

Fig. 3. Photocurrent action spectrum of SQ sensitized nanocrystalline TiO_2 electrodes. (a) Photocurrent action spectrum; and (b) absorption spectrum.

3.2. Characterization of co-adsorption of SQ and $RuL_2(NCS)_2$ on nanocrystalline TiO_2 electrodes by UV-visible absorption and IR spectra

In order to improve the light harvesting efficiency of photosensitizer, SQ can be incorporated with $RuL_2(NCS)_2$ to sensitize nanocrystalline TiO_2 electrodes. Co-adsorption of SQ and $RuL_2(NCS)_2$ was performed by dipping nanocrystalline TiO_2 electrodes in the mixture solutions with different molar proportions. The absorption spectra of the dye mixtures in ethanol solution and adsorbed on the nanocrystalline TiO_2 electrodes at molar proportion (SQ:$RuL_2(NCS)_2$) of 2:1, 1:5, 1:10, 1:20, 1;50, and 1:100 mol/mol are presented in Fig. 4. As seen from Fig. 4a, two MLCT bands in the visible and near UV of $RuL_2(NCS)_2$ and the absorption band at 646 nm of SQ are observed simultaneously in the absorption spectra of dye mixtures in ethanol solution. An intense SQ absorption band and a weaker MLCT band of $RuL_2(NCS)_2$ were presented at higher SQ concentrations, i.e. at the molar proportion of 2:1 mol/mol. The absorption band of SQ was decreased following an increase of MLCT bands of $RuL_2(NCS)_2$ when the concentration of $RuL_2(NCS)_2$ was increased such as in the molar proportions of 1:5, 1:10, 1:20, I:50: and 1:100 mol/mol. In the absorption spectra of dye mixtures adsorbed TiO_2 electrodes (Fig. 4b), the absorption bands of SQ including the monomers and the

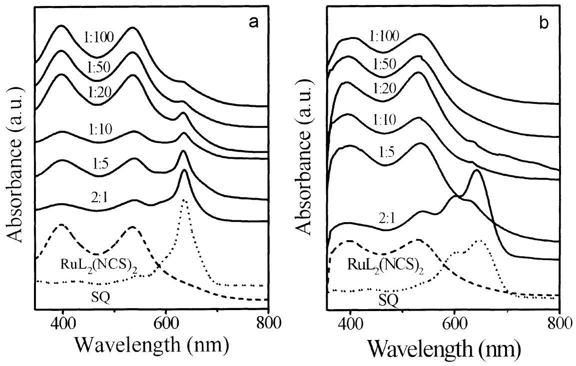

Fig. 4. Absorption spectra of the mixtures of SQ and $RuL_2(NCS)_2$ at different molar proportions: (a) in ethanol solution; and (b) adsorbed on the nanocrystalline TiO_2 electrodes.

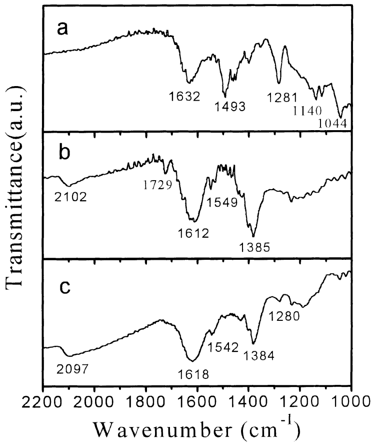

Fig. 5. Infrared spectra of dye molecules on nanocrystalline TiO_2 electrodes: (a) SQ; (b) $RuL_2(NCS)_2$; and (c) mixture of SQ and $RuL_2(NCS)_2$ in molar proportion ($SQ:RuL_2(NCS)_2$) 1:20 mol/mol.

H-type aggregates were both displayed obviously at higher SQ concentration (molar proportion of 2:1 mol/mol). It became weaker as the concentration of SQ was decreased. The absorption bands of SQ shown in Fig. 4b are less distinguishable in the high concentration of $RuL_2(NCS)_2$ as compared with Fig. 4a such as in the molar proportions of 1:50 and 1:100 mol/mol. However, the MLCT bands of $RuL_2(NCS)_2$ were increased pronouncedly with the increases of concentration of $RuL_2(NCS)_2$, resembling the absorption spectra of the dye mixtures in ethanol solution shown in Fig. 4a.

Adsorption of the mixture of SQ and $RuL_2(NCS)_2$ on the nanocrystalline TiO_2 electrode was characterized by FTIR spectra recorded in 2200–1000 cm^{-1}. Fig. 5 shows the FTIR spectra of SQ, $RuL_2(NCS)_2$ and their mixture (1:20) adsorbed on the TiO_2 electrodes. On comparison with the FTIR spectra of SQ and $RuL_2(NCS)_2$ compounds in KBr pellets, the absorption peaks in Fig. 5 could be assigned. In the FTIR spectrum of SQ (Fig. 5a), the absorption bands at 1632 and 1281 cm^{-1} were attributed to the stretch modes of the central conjugated system and $C\overset{-}{=}N$. The stretch band of indoline rings was observed at 1493 cm^{-1}. The absorptions at lower wave numbers 1140 and 1044 cm^{-1} were the symmetric and asymmetric stretch modes of $SO_3{}^-$ including $(CH_2)_3SO_3{}^-Py^+$ group, respectively. From the FTIR spectrum of $RuL_2(NCS)_2$ shown in Fig. 5b, it can be seen that SCN stretch band was at 2102 cm^{-1}. The absorption peaks at 1729, 1612 and 1549 cm^{-1} were assigned to the asymmetric stretch bands of $CO_2{}^-$ in different modes, i.e. ester-like linkage, chelating band and bridging band induced by the interaction with TiO_2, respectively. The absorption of 1385 cm^{-1} corresponded to the stretch band of pyridyl ligands. The FTIR spectrum of the dye mixture (1:20 mol/mol) adsorbed on the TiO_2 electrode is illustrated in Fig. 5c. The presence of absorption peaks of 2097, 1618, 1542 and 1384 cm^{-1} was attributed to the stretch bands of SCN, $CO_2{}^-$ and pyridyl ligands of $RuL_2(NCS)_2$, respectively, and the absorption peak at 1280 cm^{-1} was the stretch band of the central conjugated system of SQ. This FTIR spectrum provides strong evidence of the co-adsorption of SQ and $RuL_2(NCS)_2$ on nanocrystalline TiO_2 electrodes. New stretch bands cannot be found in this spectrum, indicating that the SQ and $RuL_2(NCS)_2$ co-adsorbed on the nanocrystalline TiO_2 film electrodes without chemical reactions.

3.3. Association effects of SQ and $RuL_2(NCS)_2$ on photosensitization of nanocrystalline TiO_2 electrodes

Fig. 6 is the photocurrent action spectra of nanocrystalline TiO_2 electrodes sensitized by SQ and $RuL_2(NCS)_2$ mixtures at different molar proportions. From the figure, we observe that SQ sensitized TiO_2 electrodes without $RuL_2(NCS)_2$ has low IPCE values, especially in the 400–560 nm wavelength region. After incorporating with $RuL_2(NCS)_2$ in different molar proportions, an increase of IPCE in 400–560 nm region generated by the photosensitization of $RuL_2(NCS)_2$ molecules was obtained. The IPCE values were increased with the increase of $RuL_2(NCS)_2$ concentrations. Interestingly, the IPCE values of the TiO_2 electrodes sensitized by the dye mixtures in the molar proportions of 1:20, 1:50 and 1:100 mol/mol became larger than those of $RuL_2(NCS)_2$ sensitized electrodes. This results reveal that the association effects of photosensitization of SQ and $RuL_2(NCS)_2$ occurred in the molar proportions 1:20, 1:50 and 1:100 mol/mol, resulting in the increases of IPCE. The increased IPCE of dye mixture in the molar proportion of 1:50 mol/mol was comparable to that of 1:20 mol/mol and quite larger than that of 1:100 mol/mol. Representative estimation of the improved IPCE of dye mixture with 1:50 mol/mol molar proportion shows: increases of about 19–24% in the wavelength range of 400–540 nm, 11–17% in the 550–650 nm, 1.5–9% in the 680–730 nm, and ∼1% in the 740–800 nm. Fig. 7 illustrates the dependence of IPCE of dye mixtures in the molar proportion of 1:20 and 1:50 mol/mol on the intensity of irradiated light. An increase of IPCE of dye mixtures with increasing light intensity was observed in the wavelength of 400–650 nm indicating that the enhancement effects were light-intensity dependent. The association effects of photosensitization led

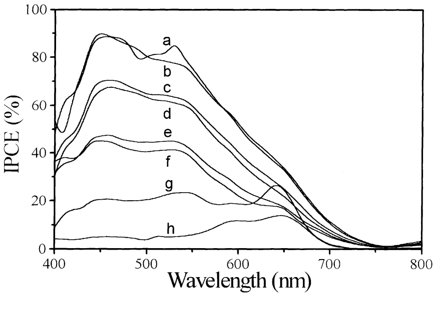

Fig. 6. Photocurrent action spectra of the mixtures sensitized nanocrystalline TiO_2 electrodes. Molar proportions ($SQ:RuL_2(NCS)_2$): (a) 1:50; (b) 1:20; (c) 1:100; (d) 0:1; (e) 1:10; (f) 1:5; (g) 2:1; and (h) 1:0.

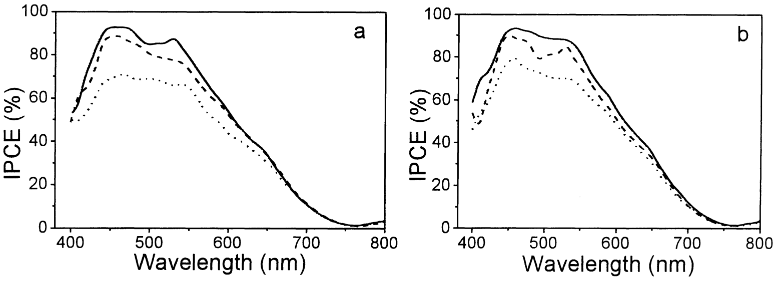

Fig. 7. The dependence of IPCE on the intensity of irradiated light. Dye mixture with molar proportions of (a) 1:20; and (b) 1:50 mol/mol. Light intensity: (—), 1.5; (- - -), 1.2; and (· · ·), 1.0 mW/cm^2.

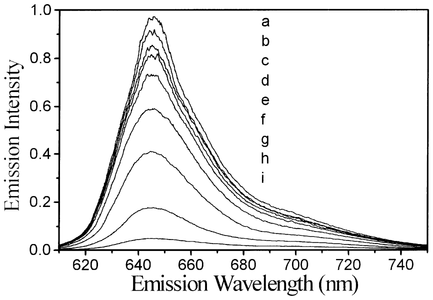

Fig. 8. Emission spectra of SQ in ethanol solution at the presence of $RuL_2(NCS)_2$. Molar proportions ($SQ:RuL_2(NCS)_2$): (a) 1:0; (b) 6:1; (c) 2:1; (d) 1:1; (e) 1:5; (f) 1:10; (g) 1:20; (h) 1:50; and (i) 1:100 mol/mol. Excitation by 590 nm light.

to improve the photoelectric behavior of the nanocrystalline TiO_2 electrodes that can be demonstrated by measuring the open-circuit photovoltages (Voc) and short-circuit photocurrents (Isc) in a thin layer cell. Table 1 lists the photoelectric response of the nanocrystalline TiO_2 electrodes sensitized by dye mixtures in different molar proportions. It can be known from the data shown in the Table 1 that the larger Vocs and Iscs were obtained in the TiO_2 electrodes sensitized by dye mixtures in molar proportions of 1:20, 1:50 and 1:100 mol/mol, corresponding to the results of IPCE observed in the photocurrent action spectra.

In order to understand the mechanism of the association effects of SQ and $RuL_2(NCS)_2$ on the photosensitization of nanocrystalline TiO_2 electrodes, the emission spectra of SQ in ethanol solution containing $RuL_2(NCS)_2$ or TiO_2 colloids were measured. Fig. 8 illustrates the emission spectra of SQ in ethanol solution in the presence of different molar proportions of $RuL_2(NCS)_2$. By exciting with 590 nm light, a strong fluorescence band centered at 646 nm was observed in the SQ emission spectra. The fluorescence intensities decreased on growing addition of the concentration of $RuL_2(NCS)_2$ implying that the fluorescence was quenched by $RuL_2(NCS)_2$ molecules. Addition of TiO_2 colloids to the SQ ethanol solution also resulted in quenching SQ fluorescence as shown in Fig. 9, in which the fluorescence intensities were suppressed gradually by the increase of concentration of TiO_2 colloids. The fluorescence quenching effects shown in Figs. 8 and 9 indicate the occurrence of electron transfer from the excited states of SQ to the $RuL_2(NCS)_2$ molecules or TiO_2 colloids. Comparison of the redox potential of SQ $E_{\mathrm{SQ}}^{-/0} \cong -1.45$ V (vs. SCE) measured from cyclic voltammetry with the redox potential of $RuL_2(NCS)_2$ $E_{\mathrm{L}}^{-/0} \cong -1.30$ V (vs. SCE) [19], the feasible electron transfer from the higher energy level of excited states of SQ to the lower energy level of $RuL_2(NCS)_2$ can be demonstrated. Based on the fluorescence quenching effects and the light intensity-dependent IPCE of dye mixtures in the molar proportions of 1:20 and 1:50 mol/mol shown in Fig. 7, it can be suggested that the electron transfer mechanism may take the responsibility for the association

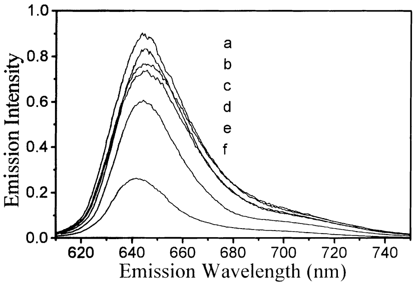

Fig. 9. Emission spectra of SQ in ethanol solution at presence of TiO_2 colloids: (a) 0.00; (b) 0.18; (c) 0.27; (d) 0.35; (e) 0.50; and (f) 0.75×10^{-3} M. Excitation by 590 nm light.

Table 1
The photoelectric performance of dye mixtures sensitized nanocrystalline TiO_2 electrodes

Dye mixture $SQ:RuL_2(NCS)_2$	Open-circuit photovoltage, Voc (V)	Short-circuit photocurrent, Isc (mA/cm^2)
0:1	0.54	10.5
1:100	0.55	11.0
1:50	0.57	12.5
1:20	0.55	12.0
1:10	0.52	9.5
1:5	0.51	9.0
1:0	0.40	2.4

effects of photosensitization of SQ and $RuL_2(NCS)_2$. An enhanced electron transfer from excited SQ to $RuL_2(NCS)_2$ led to the improvement of the photoelectric behavior of nanocrystalline TiO_2 electrodes.

4. Conclusion

Squarylium cyanine as an efficient photosensitizer in the visible red region was used to photosensitize nanocrystalline TiO_2 electrodes. Two photocurrent peaks corresponded to the absorption bands of monomers and H-type aggregates were displayed in the photocurrent action spectrum of SQ sensitized nanocrystalline TiO_2 electrodes. Photosensitization of nanocrystalline TiO_2 electrodes by co-adsorption of SQ and $RuL_2(NCS)_2$ was performed in their mixtures of different molar proportions. An increase in IPCE, Voc and Isc were obtained in the molar proportions of mixtures (SQ:$RuL_2(NCS)_2$) of 1:20,1:50 and 1:100 mol/mol. The association effects of SQ and $RuL_2(NCS)_2$ on the photosensitization of nanocrystalline TiO_2 film electrodes are attributed to the electron transfer mechanism demonstrated by SQ fluorescence quenching measurements.

Acknowledgements

This work was supported by the Dean grant of Chinese Academy of Sciences and the Photochemistry Laboratory of the Chinese Academy of Sciences.

References

[1] H. Gerischer, F. Willing, Top. Curr. Chem. 61 (1976) 31.
[2] B.A. Parkinson, M.T. Spiteer, Electrochim. Acta 37 (1992) 943.
[3] P.V. Kamat, in: J. Meyer (Ed.), Molecular Level Artificial Photosynthetic Materials. Progress in Inorganic Chemistry Series, Vol. 44, Wiley, New York, 1997, 273 pp.
[4] A. Kay, R. Humphry-Baker, M. Gratzel, J. Phys. Chem. 98 (1994) 952.
[5] N.J. Cherepy, G.P. Smestad, M. Gratzel, J.Z. Zhang, J. Phys. Chem. 101 (1997) 9342.
[6] K. Sayama, M. Sugino, H. Sugihara, Y. Abe, H. Arakawa, Chem. Lett. 320 (1998) 753.
[7] K. Norland, A. Ames, T. Taylon, Photogr. Sci. Eng. 14 (1970) 295.
[8] A. Blum, L.I. Grossweiner, Photochem. Photobiol. 14 (1971) 551.
[9] A.C. Tam, Appl. Phys. Lett. 37 (1980) 978.
[10] D.L. Morel, E.L. Stogryn, A.K. Ghosh, T. Feng, P.E. Purwin, R.F. Sjhaw, C. Fishman, G.R. Bird, A.P. Piechowski, J. Phys. Chem. 88 (1984) 923.
[11] A.P. Piechowski, G.R. Bird, D.L. Morel, E.L. Stogryn, J. Phys. Chem. 88 (1984) 934.
[12] S.D. Daleep, S.J. Shiam, J. Org. Chem. 26 (1961) 352.
[13] J. Hugo, F. Lance, J. Org. Chem. 33 (1968) 4283.
[14] L.S. Hengo, D.S. Peng, Y.Z. Chen, J.C. Li, L.Z. Yu, W.Z. Li, H.M. Zhao, J. Sichuan Univ. (Natural Sci. Edition) 32 (1995) 566.
[15] H. Kampfer, US Patent, 3 592 657 (1971).
[16] M.K. Nazeeruddin, A. Kay, I. Rodicio, R. Humphry-Baker, E. Muller, P. Liska, N. Vlachopoulos, M. Gratzel, J. Am. Chem. Soc. 115 (1993) 6382.
[17] Y-S. Kim, K. Liang, K-Y. Law, D.G. Whitten, J. Phys. Chem. 98 (1994) 984.
[18] S. Das, T.L. Thanulingam, K.G. Thamas, P.V. Kamat, M.V. George, J. Phys. Chem. 97 (1993) 13620.
[19] R. Argazzi, C.A. Bignozzi, T.A. Heimer, F.N. Castellano, G.J. Meyer, Inorg. Chem. 33 (1994) 5741.